DOI: https://doi.org/10.24425/amm.2022.141090

MIN-WOO LEE[1], YOUNG-SIN CHOI[1], DO-HUN KWON[1], EUN-JI CHA[1], HEE-BOK KANG[2], JAE-IN JEONG[2], SEOK-JAE LEE[3], HWI-JUN KIM[1*]

THE PREDICTION OF OPTIMIZED METALLOID CONTENT IN Fe-Si-B-P AMORPHOUS ALLOYS USING ARTIFICIAL INTELLIGENCE ALGORITHM

Artificial intelligence operated with machine learning was performed to optimize the amount of metalloid elements (Si, B, and P) subjected to be added to a Fe-based amorphous alloy for enhancement of soft magnetic properties. The effect of metalloid elements on magnetic properties was investigated through correlation analysis. Si and P were investigated as elements that affect saturation magnetization while B was investigated as an element that affect coercivity. The coefficient of determination R^2 (coefficient of determination) obtained from regression analysis by learning with the Random Forest Algorithm (RFR) was 0.95 In particular, the R^2 value measured after including phase information of the Fe-Si-B-P ribbon increased to 0.98. The optimal range of metalloid addition was predicted through correlation analysis method and machine learning.

Keywords: Fe-based amorphous alloy; Metalloid elements; Artificial intelligence; Coercivity; Saturation magnetization

1. Introduction

The design and development of a new alloy have long been important components of advanced engineering system. However, these processes are often too slow due to chemical and structural complexity. During the last century, ferroalloy design was essentially an empirical iteration, based on lesson learned from industrial use and human experience. Alloy design and development are costly and slow, and do not take full advantage of the data that exist in the Fe alloy metallurgy field. In the present work, an attempt to utilize a scientific approach to the data was made to develop an artificial neuron network (ANN) model for alloy design [1-2].

Fe-based amorphous alloys have been used in electric and electronics industry because of their high saturation magnetization and cost competitiveness as soft magnetic core materials [3-4]. Two conditions are required to produce excellent Fe-based amorphous alloy. The first is a very high cooling rate (>10^{-5} K/s), and the second is the large difference in atomic radius between the additive element and the matrix Fe atom. Metalloid additives like Si, B, C, and P can be located in the interstitial sites of the lattice, because of their small atomic radius [5]. They also prevent crystallization of an alloy when the alloy is cooled from liquid state to solid state [4-6]. An amorphous alloy can be produced by an appropriate combination of these elements. However, discovery of new multi-component alloy via the design through experimental route only takes a lot of time.

In this study, we tried to design an amorphous alloy of Fe-Si-B-P with the aid of artificial intelligence algorithm. In addition, we calculated the optimal combination ratio of Si, B, and P using linear regression or artificial intelligence neural network method. The amorphous forming ability (AFA) and magnetic properties (saturation magnetization and coercivity) of the alloy designed by the artificial intelligence was evaluated, and then the soft magnetic properties of the optimized Fe-Si-B-P alloy was compared with those of the actually manufactured alloy. Moreover, the correlation between each element and magnetic properties was analyzed using the Pearson correlation coefficient method.

2. Experimental

The Fe-Si-B-P alloy system was designed by changing the content of each element. The range of nominal composition (in at.%) was 79.5~85.0 Fe, 0.5~7.0 Si, 6.0~14.0 B, 1.5~4.4 P, and a total of 61 alloys were prepared. Each alloy was fabricated

[1] SMART LIQUID PROCESSING R&D DEPARTMENT OF KOREA INSTITUTE OF INDUSTRIAL TECHNOLOGY, INCHEON 21999, KOREA
[2] R&D CENTER OF YOUNGIN ELECTRONIC, YOUNGIN 1033, KOREA
[3] JEONBUK NATIONAL UNIVERSITY, DIVISION OF ADVANCED MATERIALS ENGINEERING, JEONJU 54896, KOREA

* Corresponding author: khj@kitech.re.kr

© 2022. The Author(s). This is an open-access article distributed under the terms of the Creative Commons Attribution-NonCommercial License (CC BY-NC 4.0, https://creativecommons.org/licenses/by-nc/4.0/deed.en which permits the use, redistribution of the material in any medium or format, transforming and building upon the material, provided that the article is properly cited, the use is noncommercial, and no modifications or adaptations are made.

by varying the content of Fe, Si, B, and P using an arc-melting method. The Fe-based amorphous ribbons were obtained by melt spinning with the cooling rate of 10^{-5} K/s. The dimension of the quartz tube was 20 mm in outer diameter, 17 mm in inner diameter, 160 mm in length, and the nozzle hole size was 0.5 mm. The gap distance between the wheel and the nozzle tip was set to 0.1 mm. Thermal property of the Fe-Si-B-P ribbons was analyzed using DSC (Differential Scanning Calorimetry) analysis to obtain quantitative information such as endotherm or exotherm reaction position and crystallization peaks. The heating rate was 40 K/min. in the range of 573 to 873 K during DSC analysis. The magnetic properties of the Fe-Si-B-P ribbon, such as saturation magnetization, coercivity and remanence, were measured using a vibrating sample magnetometer (VSM, LakeShore 7400 Series). The saturation magnetization and the coercivity of the ribbon specimens were measured at an applied magnetic field of 10,000 A/m.

The machine learning algorithms such as RFR (Random Forest Regression), KNN (K-Nearest Neighbor) and SVR (Support Vector Regression) were chosen to predict and to optimize the saturation magnetization and coercivity of a Fe-Si-B-P ribbon with varying metalloid elements. RFR was trained 1 to 100 decision trees. k-NN meanwhile was predicted to the average value of the nearest data used to the k nearest value, with k values ranging from 1 to 22. SVR was shown to be affected by factors C, ϒ, and ε. The set of C was 1, 10, 100, and 1000. The ϒ values were 1, 0.1, and 0.001. We used ε sets of 0.0001, 0.0005, 0.001, 0.005, 0.01, 0.05, and 0.1. A total of 61 Fe-Si-B-P amorphous ribbons were prepared and characterized. 70% of them were trained, and the remaining 30% were compared with the trained results to predict the accuracy [7-8].

3. Results and discussion

The saturation magnetization and the coercivty of 61 Fe-Si-B-P specimens are listed in Table

In general, the saturation magnetization of a soft magnetic alloy is affected by the crystal structure of the alloy and the content of the ferromagnetic element in the alloy [9]. In the case of amorphous alloys, however, the saturation magnetization is affected only by the amount of the ferromagnetic element in an alloy because there is no crystalline phase in the alloy [14-16]. As can be seen in TABLE 1, the measured value of the saturation magnetization does not change consistently with the change of Fe content in the alloys.

TABLE 1

Composition and magnetic properties like saturation magnetization and coercivity of Fe-Si-B-P amorphous ribbons

Fe-Si-B-P (at.%)	125 G	5000G	Wheel speed [m/s]
	Hc [A/m]	Ms [emu/g]	
# 1-1 $Fe_{80}Si_7B_{8.6}P_{4.4}$	35.95	177.14	36.5
# 1-2 $Fe_{80}Si_7B_{8.6}P_{4.4}$	30.85	172.61	36.5
# 1-3 $Fe_{80}Si_7B_{8.6}P_{4.4}$	35.41	172.39	36.5
# 2-1 $Fe_{82.5}Si_{6.125}B_{7.525}P_{3.85}$	44.27	170.06	36.5
# 2-2 $Fe_{82.5}Si_{6.125}B_{7.525}P_{3.85}$	138.51	178.22	36.5
# 3-1 $Fe_{85}Si_{5.25}B_{6.45}P_{3.3}$	615.68	190.03	36.5
# 3-2 $Fe_{85}Si_{5.25}B_{6.45}P_{3.3}$	435.93	191.44	36.5
# 4-1 $Fe_{80}Si_8B_8P_4$	32.09	171.02	36.5
# 4-2 $Fe_{80}Si_8B_8P_4$	35.99	170.23	36.5
# 5-1 $Fe_{82.5}Si_7B_7P_{3.5}$	111.78	174.21	36.5
# 5-2 $Fe_{82.5}Si_7B_7P_{3.5}$	53.08	171.44	36.5
# 6-1 $Fe_{85}Si_6B_6P_3$	326.99	187.07	36.5
# 6-2 $Fe_{85}Si_6B_6P_3$	303.05	188.4	36.5

This makes us difficult to predict a resultant property from experimentally designed compositions. Therefore, in order to enhance the predictability with the aid of machine learning, three machine learning algorithms were trained with the experimentally measured result.

Fig. 1 shows the result of the correlation analysis between the elements and the magnetic properties analyzed by the Pearson correlation coefficient method. The formula for the Pearson correlation coefficient (r) is as follows,

$$r = \frac{\sum_{i=1}^{n}\left(x_i-\overline{x}\right)\left(y_i-\overline{y}\right)}{\sqrt{\sum_{i=1}^{n}(x_1-\overline{x})(x_i-\overline{x})^2\sum_{i=1}^{n}\left(y_i-\overline{y}\right)^2}}$$

The Pearson correlation coefficient (r) can have a value from –1 to 1, and it is interpreted that the closer to –1, the greater the negative effect, and the closer to 1, the greater the positive effect. Also, a value close to 0 is interpreted that the effect is small [13-14]. The correlation between the saturation magnetization

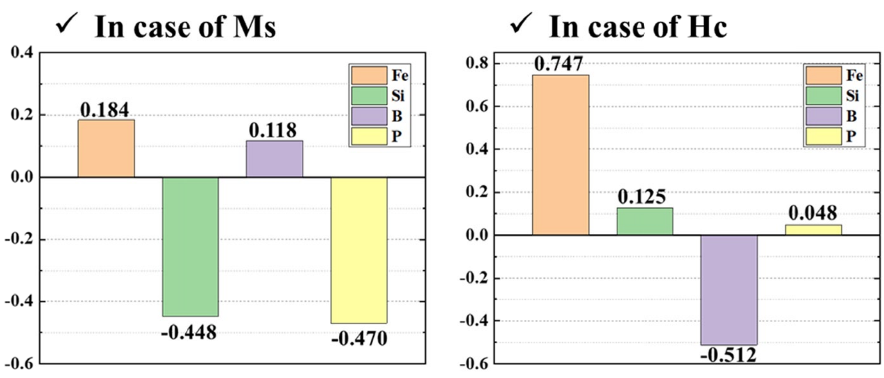

Fig. 1. The correlation between the soft magnetic properties and the metalloid elements in Fe-Si-B-P alloys using Pearson correlation coefficient

and the elements, induced from the correlation analysis result, indicated that the determined *r* value of Si and P was –0.448 and –0.470. This can be interpreted that the saturation magnetization decreases as the amount of the two elements increases. In the case of the coercivity, the determined *r* value of B was –0.512, which showed the highest correlation among the metalloid elements. It thus implies that the coercivity will increase with the increase of B content in the alloy.

Fig. 2 shows the range of data used in the machine learning algorithm and the execution condition of each algorithm. The input data was the range of Fe, Si, B, and P content, and the output data was the coercivity and the saturation magnetization. Because all of the prepared ribbons were not amorphous, phase information was also included in the data in order to distinguish the phases.

Fig. 3 shows the result of the regression analysis of RFR, KNN, and SVR. R^2 values are shown at the top left of the graphs. The R^2 value is the coefficient of determination which is the ratio of the dependent variables that can be explained by the independent variables in the regression model.

The R^2 has a value between 0 to 1 and gets closer to 1 as the relationship between the independent variables and the dependent variables increases [13-14]. In terms of the coercivity, as shown in Fig. 3(a), the R^2 value measured by machine learning with each algorithm was 0.95 for RFR, 0.93 for KNN, and 0.68 for SVR, respectively. RFR and KNN showed accuracy more than 90%. In particular, RFR showed the highest R^2 value. For saturation magnetization, the R^2 value measured by machine learning with each algorithm was 0.66 for RFR, 0.54 for KNN, and 0.58 for SVR, respectively. Therefore, the RFR algorithm also yields the highest R^2 value for the saturation magnetization but its accuracy is far lower than that for the coercivity, resulting in about 20% discrepancy. In order to improve the accuracy of the regression analysis, the collected data was classified into crystalline phase and amorphous phase. For the classification, the ribbon alloys having a coercivity of 50 A/m or less were classified as amorphous ribbons, and the crystalline phase was designated as 1 while the amorphous one is designated as 0. Fig. 3(b) shows the result of regression analysis after such phase information was added. The R^2 value for the coercivity was increased to 0.98 in the case of RFR, which is the highest one, with the addition of the phase information. Even for SVR, which showed the most inaccurate result for the coercivity, the accuracy was improved about 16% when the phase information was added. The accuracy of the analysis for the saturation magnetization was also increased about 13% after the addition of the phase information.

Fig. 4 shows the result predicted by the RFR algorithm learned with the data in which phase information is included. When alloys were designed, the saturation magnetization and the coercivity were predicted after setting the range of element addition from the minimum to the maximum amount. From the result of correlation analysis, it was found that Si has somewhat negative effect on saturation magnetization, showing slight reduction of saturation magnetization with 3~4 at.% Si. B was

Input data	Range [at.%] Min.	Range [at.%] Max.	Output data
Fe	79.5	85.0	
Si	0.5	7.0	
B	6.0	14.0	y_1 = Hc
P	1.5	4.4	y_2 = Ms
Phase information	0 : amorphous 1 : crystalline		

◆ **Initial data : 61, train : 70 %, test : 30 %,**
- RFR : 10~100 tree
- KNN : 1~36 data
- SVR : ε 0.1~0.0001, C = 100, γ = 0.1

  kernel : radial basis function(rbf)

Fig. 2. Fig. 2. Composition range of Fe-Si-B-P alloy system used in machine learning and prediction conditions of each algorithm

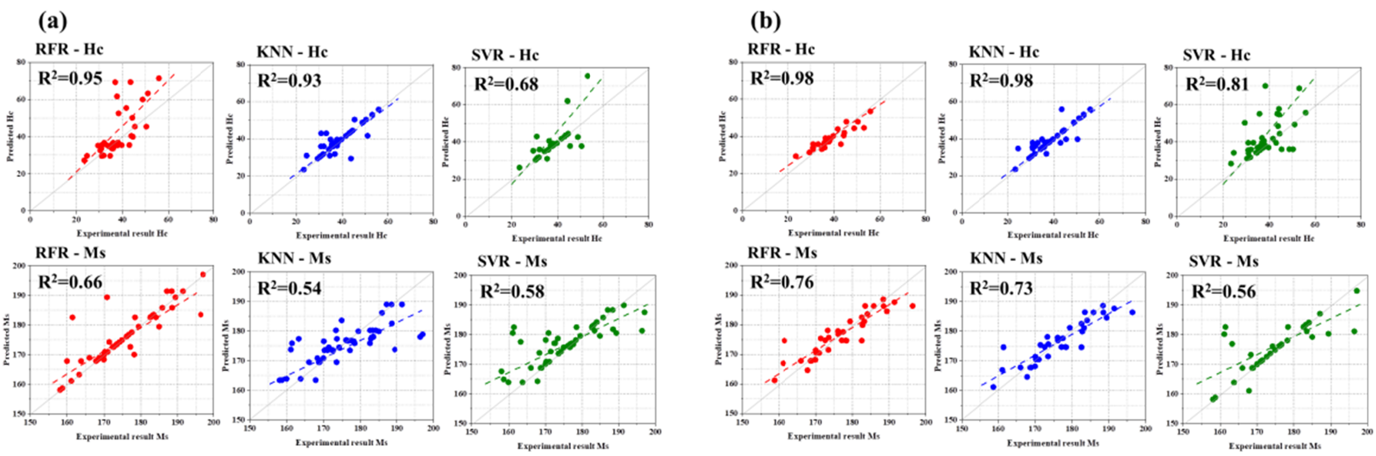

Fig. 3. The results of regression analysis with RFR, KNN, and SVR (a) and the results after adding the additive phase information (b)

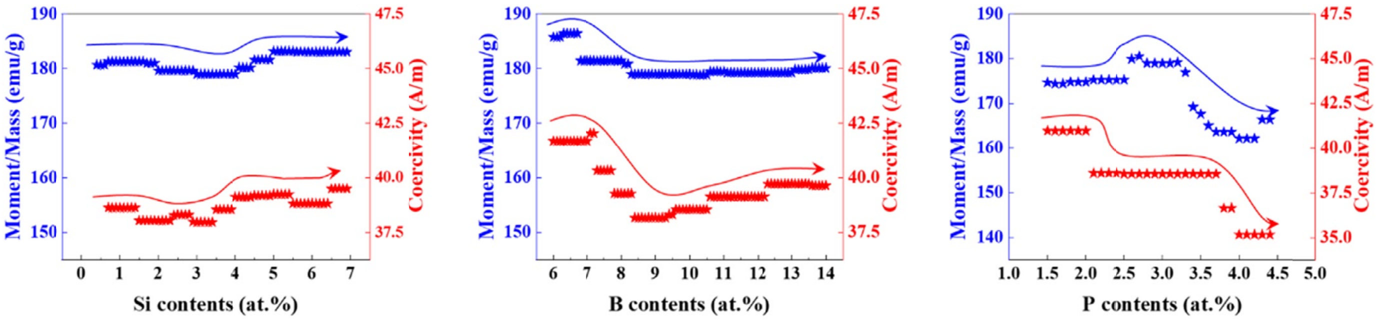

Fig. 4. The dependence of soft magnetic properties on the amount of metalloid Si, B, and P predicted by the RFR algorithm

found to be effective for reduction of the coercivity, by decreasing the coercivity when the addition of B was 6~9 at.%. However, the coercivity increased again when the amount of B exceeded 9 at.%. Meanwhile, P was predicted to have a harmful effect on saturation magnetization. Saturation magnetization decreased as the amount of P addition increased.

TABLE 2

The candidate compositions of Fe-Si-B-P alloy predicted by RFR machine learning algorithm

Input data		**Predicted quantity of element [at.%]**				**Measured data**	
Hc [A/m]	**Ms [emu/g]**	**Fe**	**Si**	**B**	**P**	**Hc [A/m]**	**Ms [emu/g]**
40	175	bal.	2.64	8.85	4.11	42.01	170.87
50	175	bal.	3.32	9.05	4.14	49.57	170.09

TABLE 2 shows predicted alloy compositions derived from the RFR algorithm learned with input data of saturation magnetization and coercivity. By the correlation analysis and machine learning prediction, it was possible to predict the composition range of metalloid elements and their effect on magnetic properties. A ribbon of the predicted composition was prepared and the magnetic properties were measured. As a result, the coercivity was almost similar value compare with input data. However, the saturation magnetization showed a difference of about 5 emu/g from input data. The reason for the difference between the predicted value and the measured value of saturation magnetization was that the machine-learned R^2 value was rather low at 0.76 (RFR).

4. Conclusions

In this study, the composition of Fe-Si-B-P alloy system was designed with the aid of machine learning algorithms. The relationship between the magnetic properties, i.e., saturation magnetization and coercivity and the amount of metalloid elements in the alloys was predicted through the Pearson correlation coefficient. An algorithm to predict the saturation magnetization and the coercivity was trained using three types of artificial intelligence. The predicted value of the coercivity was almost similar to the experimental data. R^2 values was 0.98 in RFR method. Through RFR machine learning, it was possible to obtain an amorphous composition with desired soft magnetic properties. In the next study, the Fe-Si-B-P alloys whose metalloid contents were predicted by the algorithms using artificial intelligence will be made and characterized their magnetic properties.

REFERENCES

[1] J.H. Jeon, N. Seo, H.J. Kim, M.H. Lee, H.K. Lim, S.B. Son, S.J. Lee, Metals **11**, 729 (2021).

[2] J.H.N. Seo, S.B. Son, S.J. Lee, M. Jung, Metals **11**, 1159 (2021).

[3] A. Inoue, T. Zhang, A. Takeuchi, Appl. Phys Letters **71**, 105 (1997).

[4] F.E. Luborsky, Handbook of Ferromagnetic Materials **1**, 451-529 (1980).

[5] C. Suryanarayana, A. Inoue, Bulk Metallic Glass **12**, 55, 469 (2011).

[6] B.L. Shen, M. Akiba, A. Inoue, Appl. Phys Letters 88, 131907 (2006).

[7] Z. Jie, A. Julian Morris, Neural Network **11**.1 65-80 (1998).

[8] I.M. Monirul, K. Murase, Neural Network **14**.9, 1265-1278 (2001).

[9] B.L. Shen, M. Akiba, A. Inoue, Appl. Phys Letters **88**, 131907 (2006).

[10] M. Mitera, M. Naka, T. Masumoto, N. Kazama, K. Watanabe, Physica Status Solids **(a) 49**, K163-K165 (1978).

[11] B. Shen, A. Inoue, Materials Transactions **43**, 1235-1239 (2002).

[12] M. Zou, S. Meng, Q. Li, H. Li, C. Chang, Y. Sun, Intermetallics **83**, 83-86 (2017).

[13] K. Fazil, International Journal of Electrical Powder & Energy System **67**, 431-438 (2015).

[14] W. Wen, Z. Hao, X. Yang, Neurocomputing **71**, 3096-3103 (2008).